HARMONI at ELT: project status and instrument overview

Niranjan Thatte, Dave Melotte, Benoît Neichel, David Le Mignant, Philip Rees, Fraser Clarke, Vanessa Ferraro-Wood, Oscar Gonzalez, Maia Jones, Alonso Álvarez Urueña, et al.

HARMONI at ELT: Project status and Instrument Overview

Niranjan A. Thatte*[a], Dave Melotte[b], Benoit Neichel[c], David Le Mignant[c], Phil Rees[b], Fraser Clarke[a], Vanessa Ferraro-Wood[a], Oscar Gonzalez[b], Maia Jones[b], Alonso Álvarez Urueña[e], Heribert Argelaguet Vilaseca[e], Santiago Arribas[e], José Antonio Caballero[e], Gonzalo José Carracedo Carballal[e], Alberto Estrada Piqueras[e], Irene Ferro[e], Miriam García García[e], Isabella Lamperti[e], Miguel Pereira Santaella[e], Michele Perna[e], Javier Piqueras Lopez[e], Nicolas Bouché[f], Didier Boudon[f], Eric Daguise[f], Nicola Domenis[f], Jérémy Fensch[f], Olivier Olivier Flasseur[f], Rémi Giroud[f], Matthieu Guibert[f], Aurelien Jarno[f], Alexandre Jeanneau[f], Jens-Kristian Krogager[f], Maud Langlois[f], Florence Laurent[f], Magali Loupias[f], Jean-Emmanuel Migniau[f], Dieu Nguyen[f], Laure Piqueras[f], Alban Remillieux[f], Johan Richard[f], Arlette Pecontal[f], Lisa Bardou[g], David Barr[g], Sylvain Cetre[g], Sofia Dimoudi[g], Marc Dubbledam[g], Andrew Dunn[g], Dimitri Gadotti[g], Joss Guy[g], David King[g], Anna McLeod[g], Simon Morris[g], Tim Morris[g], Kieran O'Brien[g], Emily Ronson[g], Russell Smith[g], Lazar Staykov[g], Mark Swinbank[g], Matteo Accardo[h], Domingo Alvarez Mendez[h], Pablo Alberto Fuerte Rodriguez[h], Elizabeth George[h], Derek Ives[h], Leander Mehrgan[h], Eric Mueller[h], Javier Reyes[h], Ralf Conzelmann[h], Pablo Gutierrez Cheetham[h], Angel Alonso Sanchez[i], Giuseppina Battaglia[i], Miguel Cagigas[i], Julio A. Castro-Almazán[i], Haresh Chulani[i], Graciela Delgado García[i] , Patricia Fernandez Izquierdo[i], Donaji Esparza-Arredondo[i], Begoña García-Lorenzo[i] , Alberto Hernández González[i], Elvio Hernandez Suarez[i], Javier Licandro[i], Enrique Joven[i], Roberto López López[i], Alejandro Antonio Lujan Gonzalez[i], Yolanda Martín Hernando[i], Ignacio Martín-Navarro[i], Evencio Mediavilla[i], Saúl Menéndez Mendoza[i], Luz Maria Montoya Martínez[i], José Peñate Castro[i], Felipe Murgas[i], Enric Pallé[i], Álvaro Pérez[i] , Jose Luis Rasilla[i], Rafael Rebolo[i], Horacio Rodríguez[i], Luis Fernando Rodríguez Ramos[i], Victor Sánchez Béjar[i], Tariq Shahbaz[i], Afrodisio Vega Moreno[i], Teodora Viera[i], Mickaël Bonnefoy[j], Tony Bret[j], Alexis Carlotti[j], Jean-Jacques Correia[j] , Stéphane Curaba[j], Alain Delboulbe[j], Sylvain Guieu[j], Adrien Hours[j], Zoltan Hubert[j], Laurent Jocou[j], Yves Magnard[j], Laurence Michaud[j], Thibaut Moulin[j], Fabrice Pancher[j], Patrick Rabou[j], Sylvain Rochat[j], Eric Stadler[j], Thierry Contini[k], Marie Larrieu[k], Sébastien Mamessier[k], Olivier Boebion[l], Yan Fantei-Caujolle[l], Daniel Lecron[l], Philippe Amram[c], Patrick Blanchard[c], William Bon[c], Anne Bonnefoi[c], Alexandre Bozier[c], William Ceria[c], Zalpha Challita[c], Yannick Charles[c], Elodie Choquet[c], Anne Costille[c], Audrey Delsanti[c], Kjetil Dohlen[c], Franck Ducret[c], Kacem El Hadi[c], Benjamin Foulon[c], Jean-Luc Gimenez[c], Olivier Groussin[c], Marc Jaquet[c], Edgard Renault[c], Paul Rouquette[c], Patrice Sanchez[c], Arthur Vigan[c], Annie Zavagno[c], Romain Fetick[c,d], Thierry Fusco[c,d], Cedric Héritier[c,d], Jean-Francois Sauvage[c,d], Nicolas Vedrenne[c,d], Demet Aksoy[m], Martin Caldwell[m], Ann Fitzpatrick[m], Carl Geddert[m], Peter Hiscock[m], Emma Johnson[m], Murali Nalagatla[m], Louise Saraff[m], Joe Shreeves[m], Matthew Tildesley[m], Mark Wells[m], Anastasios Aretos[b], Lee Barrett[b], Martin Black[b], Charlotte Bond[b], Saskia Brierley[b], Ian Bryson[b], Amelia Calderhead[b], Kenny Campbell[b], James Carruthers[b], Lee Chapman[b],William Cochrane[b], Rory Gillespie[b], Joel Harman[b], Douglas Harvey[b], Eamonn Harvey[b], Bethany Johnson[b], Tom Louth[b], Mike MacIntosh[b], Anna MacIver[b], Chris Miller[b], David Montgomery[b], Meenu Murali[b], John Murray[b], Norman O'Malley[b], Ruben Sanchez-Janssen[b], Noah Schwartz[b], Patrick Smith[b], Jonathan Strachan[b], Stephen Todd[b], Dawn Wasley[b], Sandi Wilson[b], Junyi Zhou[b], Eric Bell[n], Oleg Gnedin[n], Kayhan Gultekin[n], Mario Mateo[n], Michael Meyer[n], Jayne Birkby[a], Liam Boland[a], Michele Cappellari[a], Edgar Castillo Dominguez[a], David Gooding[a], Kearn Grisdale[a], Andrea Hidalgo[a], James Kariuki[a], Ian Lewis[a] , Kieran McCall[a], R. Elliot Meyer[a], Eduard Muslimov[a], Adam Lowe[a], Zeynep Ozer[a], Sophie Paszynska[a], Dimitra Rigopoulou[a], Matthias Tecza[a], Alec York[a].

Ground-based and Airborne Instrumentation for Astronomy X, edited by Julia J. Bryant, Kentaro Motohara, Joël R. D. Vernet, Proc. of SPIE Vol. 13096, 1309614
 · 0277-786X · doi: 10.1117/12.3018520

[a]Dept. of Astrophysics, University of Oxford, Keble Road, Oxford, OX1 3RH, U.K.; [b]UKATC, Royal Observatory Edinburgh, Blackford Hill, Edinburgh, EH9 3HJ, U.K.; [c]Laboratoire d'Astrophysique de Marseille, 38, rue Frédéric Joliot-Curie, 13388 Marseille cedex 13, France; [d]ONERA, B.P.72, 92322, Chatillon, France; [e]Centro de Astrobiologica (CSIC/INTA),28850 Torrejón de Ardoz, Madrid, Spain; [f]CRAL, Observatoire de Lyon, 9 Avenue Charles Andre, 69561 Saint Genis Laval, France; [g]Department of Physics, Durham University, South Road, Durham DH1 3LE, U.K.; [h]ESO, Karl-Schwarzschildstrasse 2, 85748, Garching, Germany; [i]IAC, C/ Via Lactea, s/n, 38205, La Laguna (Tenerife), Spain; [j]Institut de Planétologie et d'Astrophysique de Grenoble, 414, Rue de la Piscine, 38400 St-Martin d'Hères, France.; [k]Observatoire Midi-Pyrénées, 14 avenue Edouard Belin, 31400 Toulouse, France; [l]Institut LAGRANGE, Observatoire de la Côte d'Azur, Boulevard de l'Observatoire, CS 34229 – F 06304 Nice, Cedex 4, France.; [m]RAL Space, STFC, Rutherford Appleton Laboratory, Didcot OX11 0QX, U.K.; [n]University of Michigan, 1085 S. University, 323 West Hall, Ann Arbor, MI 48109-1107, U.S.A.

ABSTRACT

HARMONI is the first light visible and near-IR integral field spectrograph for the ELT. It covers a large spectral range from 450 nm to 2450 nm with resolving powers from 3500 to 18000 and spatial sampling from 60 mas to 4 mas. It can operate in two Adaptive Optics modes - SCAO (including a High Contrast capability) and LTAO - or with NOAO. The project is preparing for Final Design Reviews. HARMONI is a work-horse instrument that provides efficient, spatially resolved spectroscopy of extended objects or crowded fields of view. The gigantic leap in sensitivity and spatial resolution that HARMONI at the ELT will enable promises to transform the landscape in observational astrophysics in the coming decade. The project has undergone some key changes to the leadership and management structure over the last two years. We present the salient elements of the project restructuring, and modifications to the technical specifications. The instrument design is very mature in the lead up to the final design review. In this paper, we provide an overview of the instrument's capabilities, details of recent technical changes during the red flag period, and an update of sensitivities.

Keywords: integral field spectroscopy, adaptive optics, ELT, image slicer, high contrast

1. INTRODUCTION

HARMONI will provide the Extremely Large Telescope's (ELT) workhorse spectroscopic capability at visible and near-infrared wavelengths, commencing soon after first light. The instrument is an integral field spectrograph (hyper-spectral imager) that provides, in a single exposure, simultaneous spectroscopy of every spatial pixel (spaxel) in a ~200×150 spaxel contiguous field-of-view with near 100% fill factor. Assisted by adaptive optics (AO), it provides near-diffraction limited spatial resolution (~12-15 milli-arcseconds) over most of the sky, with even higher Strehl ratios achieved when a sufficiently bright natural star is within ~10 arc seconds of the science target, and can be used as a reference. It also has a high contrast mode, suitable for direct imaging, spectroscopy and characterisation of extra-solar planets.

Each exposure results in a data cube of observed flux as a function of two spatial coordinates in the plane of the sky, and a spectral (wavelength) coordinate. HARMONI's high throughput and large detector real estate (8 H4RG array detectors) ensure efficient, point-and-shoot spectroscopy without slit losses, or slit positioning uncertainty. The information from each data cube can be analysed to derive morphological, kinematic and dynamical properties of the target object [2][5]. The use of emission / absorption line ratios can also yield chemical abundance information, as well as physical parameters such as temperature, density and ionization state [2][9].

2. INSTRUMENT OVERVIEW

HARMONI's capabilities and instrument architecture are largely unchanged since 2020, and have been described in some detail in past SPIE conference proceedings [6] [7]. For completeness and to aid understanding, we provide a brief summary of the instrument capabilities and a summary description of the instrument in the paragraphs below.

HARMONI is an AO assisted visible and near-infrared integral field spectrograph for the ESO ELT. It provides four spaxel scales of 60×30, 20×20, 10×10, and 4×4 milli arcsec, with corresponding fields of view of 152×204 spaxels in each setting. Spectral coverage is in the wavelength range: 0.47 to 2.45μm, provided by 11 Volume Phase Holographic Gratings (VPHG), one covering the visible (0.47 to 0.82 μm) at R~3000, while the other ten VPHG cover the near-IR at resolving powers of *R*~3500, 7000 & 17000, at all spaxel scales. The spectra are Nyquist sampled (2.2 pixels per resolution element) and the common wavelength range for any grating setting is about 3300 pixels. The instrument is designed for excellent throughput, low thermal background, and the image quality preserves the exquisite (diffraction-limited) spatial resolution provided by the ELT and HARMONI's AO systems.
Both spaxel scale and grating can be chosen "on-the-fly". The four spaxel scales are optimized for maximal FoV (60×30 mas), best sensitivity (20×20 mas and 10×10 mas), or to Nyquist sample the diffraction limit of the ELT (4×4 mas). The design challenge for the coarsest spaxel scale is to focus the light from the enormous ELT collecting area into a 15×15 μm detector pixel, whilst maintaining excellent image quality. The aspect ratio of the FoV is well suited to "nodding-on-IFU", a popular observing strategy that yields good sky background subtraction.

The HARMONI Integral Field Spectrograph's (IFS) capabilities are enhanced by the instrument's adaptive optics (AO) systems, all of which use the ELT's own M4 deformable mirror and M5 fast tip-tilt mirror as the corrective elements in the adaptive optics path. Laser Tomographic Adaptive Optics (LTAO) uses light from six Laser Guide Star (LGS) reference sources, together with two natural guide stars (NGS) within a 1 arc minute radius technical field to sense the wavefront aberrations and send corrections to the ELT's M4-M5 via the Real Time Computer (RTC). LTAO provides excellent sky coverage with near diffraction-limited performance. Even better performance (higher Strehl ratios) can be obtained when a single bright natural guide star is available. The Single Conjugate Adaptive Optics (SCAO) sensing system can accommodate a guide star up to 15 arc seconds from the IFS field centre. The High Contrast Adaptive Optics (HCAO) mode is a subset of the SCAO mode – it uses on-axis bright natural stars as a reference, and additional wavefront sensors and pupil plane apodisers to provide contrasts of 10^{-6} (after post-processing) at 100 mas from the star. HCAO is planned to be used for exoplanet characterization.

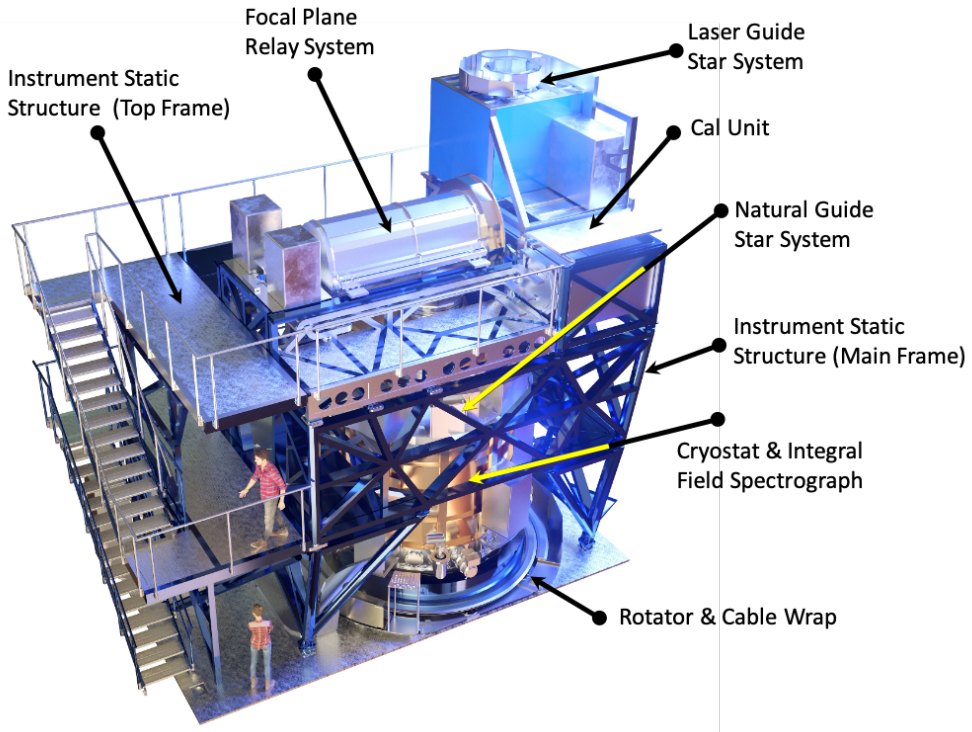

Figure 1: CAD layout of the HARMONI instrument, located on the ELT's Nasmyth platform, with the major sub-systems identified.

The figure above shows a schematic layout of the HARMONI instrument, that helps to identify its major systems and sub-systems. HARMONI is hosted at the side looking port on the ELT Nasmyth platform, light from the telescope's M6 folding mirror enters the instrument at the top right of the figure, 6 meters above the platform. Light enters the Focal Plane Relay System (FPRS), which together with the Calibration Unit make up the Calibration and Relay System (CARS) of the instrument. Laser light is reflected off the laser dichroic at the entrance to the FPRS to the Laser Guide Star System (LGSS) located at the top of the instrument, with its own de-rotator to track the laser star spots, which move with the pupil. The output of the FPRS is directed vertically downwards towards the Integral Field Spectrograph (IFS), located in an upward looking, 3.5 meter diameter, cryostat. The cryostat is mounted on the platform via the Instrument Rotator and Wrap, and rotates about a vertical axis to compensate for field rotation. The IFS cryostat houses the Pre-Optics (IPO), the Integral Field Unit (IFU), and the four spectrographs (ISP), with the associated science detectors. The vertical rotation axis guarantees an invariant gravity vector, improving the instrument's stability by minimizing flexure. The Natural Guide Star System (NGSS) is located on top of the IFS cryostat, and co-rotates with it. It houses all the natural guide star sensors. The Instrument Static Structure (ISS) provides a robust mechanical structure and access to all instrument systems.

3. RED FLAG AND RESULTING CHANGES

The HARMONI Project has been under *special measures* for a period of two years, from Sep 2021 when ESO raised a 'Red Flag' until it was lifted at the end of 2023. During these two years, the project underwent a number of changes, both technical and managerial. We present some details of the key technical changes below.

Technical Changes

As a result of detailed analysis carried out by the various task forces set up during the red flag process, and subsequent discussions between ESO and HARMONI Consortium, a number of changes to the instrument design were agreed. Chief amongst them are the following:

1. Change of FPRS and NGSS temperature from -15°C to +2°C.
2. Addition of a second NGS probe arm to better constrain the IFS field-of-view's World Coordinates.
3. Adoption of an alternative design for the spectrograph IR cameras, excluding ZnSe.

These are detailed in the following sub-sections. Several of the changes have an impact on instrument performance and expected sensitivity. The updated sensitivity tables are presented in the next section.

3.1 Change of FPRS and NGSS Temperature

This change is an outcome of the HARMONI red flag process, specifically MI-002 from "TF7" on FPRS-NGSS temperature. The recommended change by the TF7 committee is to increase the FPRS temperature to +2°C (from -15°C). The FPRS and NGSS in HARMONI have 9–11 optical surfaces (depending on AO operational mode) compared to the telescope's 6 surfaces (for an instrument at the side-looking Nasmyth port). Despite being easier to keep clean than the exposed telescope mirrors, the instrument's reflective surfaces must be colder than the telescope to avoid introducing an overwhelming amount of additional thermal background.

It is worth noting that in all cases we plan to operate at a fixed temperature, to aid stability in the NGSS sub-system. Whilst it is seen as technically feasible to work at -15°C as proposed, operating at +2°C is seen as considerably less risky for both the project and the observatory. In particular:

- The risk of ice formation (either inside or outside the FPRS/NGSS volume) due to leaks is removed.
- The risk of condensation forming on the outer skin of the FPRS/NGSS due to thermal bridges is reduced.
- The power required to cool the volumes is reduced, and may allow the removal of one of the chillers.
- Schedules during AIT can be reduced by an estimated 4 months.
    - Fewer environmental verification tests to undertake
    - Shorter integration / test cycle time
- Access times in case of maintenance are reduced (shorter warm-up/cool-down time).

- High performance mechanisms operating at +2°C are commercially available.

This increased background translates to a loss of K-band sensitivity of approximately 0.16 magnitudes in the most affected operational configurations (60x30mas, R=3500 LR2 (H+K) grating). This corresponds to a 34% increase in observing time for K band exposures to achieve the same SNR. Below 2 μm, the temperature of the FPRS/NGSS has little/no impact on limiting sensitivity. Observations in the 4 mas scale are less affected, as these remain read-noise limited even in the longest reasonable exposure times (900s).

The telescope itself is still the major contributor to the total thermal background. Sensitivity can then be recovered to some extent by scheduling sensitive K-band observations on cold nights. The sensitivity of the -15°C solution in median conditions (+9°C ambient) is recovered with the +2°C solution for ambient temperatures below ~5°C. This, of course, comes at the cost of observability as only 10% of the nights on Armazones will have Tambient < +5°C. With these potential mitigations, the project science teams have validated the FPRS-NGSS temperature change as acceptable.

3.2 Addition of a second NGS Probe arm

Given the HARMONI IFS's modest field of view, the majority of HARMONI's science exposures do not contain a point like (or sufficiently compact) object within the science field that can be used to define the World Coordinate System (WCS) of the long exposure. Instead, HARMONI relies on the Natural Guide Star (on-axis or near on-axis for SCAO mode, off-axis for LTAO mode) coordinates, and accurate knowledge of the NGS probe arm (when using LTAO) relative to the IFS field centre to establish the WCS for the latter. However, as shown schematically in the figure below, any changes in telescope plate scale (radial w.r.t. the NGS) or field rotation angle knowledge (azimuthal w.r.t. the NGS) result in IFS field centre motion. This has two consequences: (1) variations in plate scale and field rotation angle during the long exposure cause an additional blurring of the long exposure PSF and (2) errors in knowledge of the average value of plate scale and field orientation lead to inaccuracies in the WCS knowledge for the IFS field centre. Detailed analysis showed that both these effects were large enough to disrupt compliance with the HARMONI top level requirements.

The telescope is unable to guarantee field *orientation* – i.e. the apparent angle of 'North' at the Nasmyth adaptor – to a level better than 30 mas/arcminute (0.18 degrees). This term is in addition to the field rotation contribution to the field aberrations term given in the ICD. An error in field orientation at the start of the exposure maps into a pointing error and affects the WCS knowledge. *Changes* in field orientation error during an exposure affect image quality. We model the field orientation error as an error in the starting point of the trajectory of the telescope. If the starting position (hour angle or declination) is wrong, the trajectory we follow throughout the exposure will be slightly wrong, leading to a degradation in image quality during the exposure. Over much of the sky, the trajectory error is a small contributor to long exposure image quality. Around zenith however, a significant fraction of the observations would be affected by this. The field orientation term could dominate for observations with ~15 degrees of the Zenith.

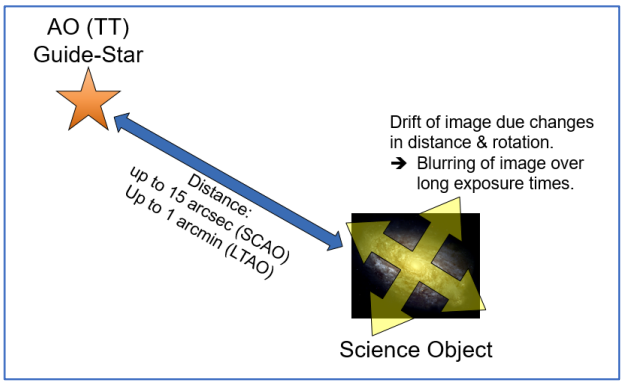

Figure 2: Schematic showing the effects of plate scale and field rotation errors on the IFS field of view (field centre motion and image blurring) – courtesy F. Clarke

The conclusions of a detailed analysis of controlling both WCS knowledge and image quality to sufficient accuracy to satisfy the instrument top level requirements was to introduce a second NGS probe arm that would constrain both parameters. The introduction of the second NGS probe was agreed with ESO during the red flag process, and a significant

modification to the instrument design has been undertaken to accommodate the two NGS solution. This has resulted in the NGS probe arms being re-designed, and has provided benefits to the accessibility and maintainability of the NGS system.

A comprehensive analysis of the impact of the two NGS probe arm re-design is shown in the figure below. It demonstrates that both the WCS knowledge requirement (left hand plot) and the image quality requirement (right hand plot) can be easily met with the two NGS solution that is currently being implemented.

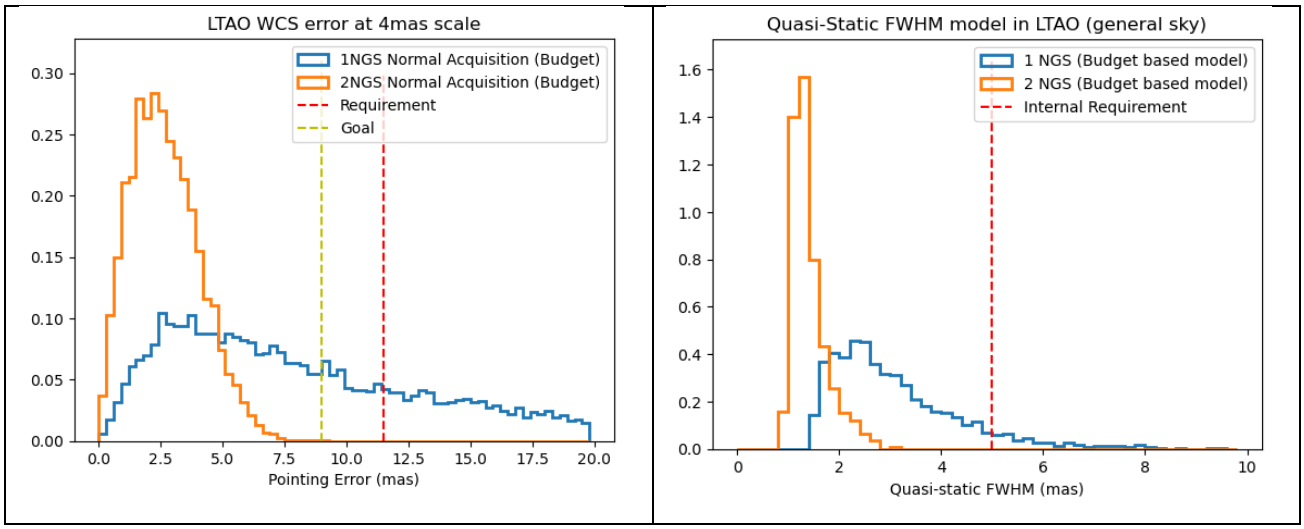

Figure 3: Plots showing the impact of using 1 vs. 2 NGS on the WCS knowledge (left hand panel) and the image blurring (right hand panel). Plots courtesy of F. Clarke.

3.3 Alternative Spectrograph IR camera design

The HARMONI IFS is composed of four identical spectrograph units, located within the main IFS cryostat, at an operating temperature of 130 K. Each spectrograph disperses a 500 mm long slit on to a pair of H4RG near-IR detector arrays. A spectrograph unit is composed of an all-reflective three element collimator, a Volume Phase Holographic Grating (VPHG) disperser, and a refractive multi-element camera. Ten VPHG are located on a grating wheel allowing a choice of spectral resolving power and instantaneous wavelength coverage. Fold mirror mechanisms ensure that the angle of incidence for all gratings satisfies the Bragg condition to ensure maximum efficiency. Optionally, the fold mirrors allow light to be directed to a single fixed grating matched to the visible wavelength range. Light dispersed by the VIS grating is focused by a second, visible camera on to a pair of $4k^2$ CCD detector arrays, whose size matches the H4RG near-IR detectors. Only two of the spectrographs will be equipped with the visible channel.

The baseline near-IR camera design stems from 2020, and is shown in the left hand figure below. The optical design has 7 elements with one aspheric surface. The materials used are CaF_2 (3 elements), ZnSe (2 elements), Suprasil 3001 (1 element) and glass S-FTM16 (1 element). The design was analyzed in detail and found to be compliant in all requirements except the bulk scattering requirement. The non-compliance stems from the two ZnSe components located close to the detector arrays.

The near-IR sky background is dominated by a large number of highly variable, narrow, night sky airglow emission lines – e.g. the H band has about 80 such strong lines, which are unresolved even at the highest spectral resolving power provided by HARMONI. The night sky emission is very faint in between these bright emission features, thus offering ground based observations the possibility of superb sensitivity (very low sky background) in these “dark areas in between the night sky emission lines”. However, to achieve the best sensitivity afforded by these dark gaps in wavelength, the instrument must fulfil tight constraints on all other noise sources, such as detector noise. A limiting feature of the baseline camera design was the enhanced spectral scatter, causing flux from the bright night sky lines to be scattered into the neighbouring dark gaps. Consequently, as part of the red flag process, several other camera designs were explored, and a trade-off analysis was performed to select the best option.

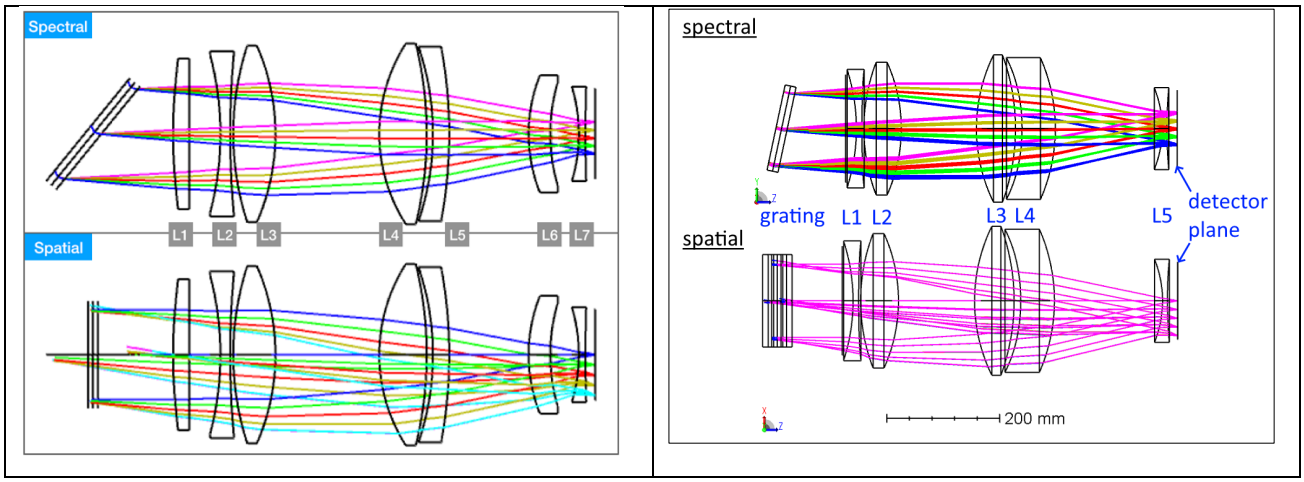

Figure 4: Schematic of the 7 lens spectrograph camera design (left hand panel), and the newer 5 lens camera design that does not use ZnSe (right hand panel).

The new adopted design is shown in the right hand panel of the figure above. It consists of only five elements, and the glasses used are S-FTM16, CaF_2 and Suprasil 3001. Apart from superior bulk scattering performance, the five element design is also expected to provide better throughput because of the lower surface count, lower manufacturing costs and ease of assembly and alignment. The drawbacks are that two surfaces require aspheric figures, while the baseline design has only one. Even with the added asphere, the wavefront error performance of the five element camera is substantially worse than that of the baseline design. However, the trade-off study established that despite the worse wavefront error performance, the overall image quality specifications of the spectrograph units could be met with the five lens design. Consequently, it was adopted as the preferred choice for the spectrograph near-IR cameras.

4. INSTRUMENT SENSITIVITY

The instrument's point-source and extended source sensitivity is a single number that provides the end-user with a direct estimate of the expected performance, and is a good metric to track the impact of design changes on proposed observing programmes. HARMONI's sensitivity is defined as the brightness of a point or extended source to achieve a signal-to-noise ratio of five per spectral resolution element in the extracted spectrum of an astronomical source, in five hours (20×900s) of on-source exposure time. However, we recognise that the achieved sensitivity depends on a large number of factors, some of which are directly impacted by the instrument design (e.g. instrument throughput), and others that are not (e.g. atmospheric seeing). Nonetheless, it is valuable from a scientific viewpoint, to use these technical requirement specifications to estimate the expected sensitivity of HARMONI to help the end user (and scientific oversight committees) to gain a feel for what might be achievable in terms of signal-to-noise ratio (SNR) for planned observations with HARMONI at the ELT.

We computed sensitivities via two methods: 1) using a spreadsheet based ETC and 2) using the HARMONI simulator `HSIM` [4][8]. This allowed us to cross check both results to give us confidence in our methodologies. Both tools are complementary, with the ETC allowing a very quick analysis of changes in technical parameters, whilst `HSIM` [4][8] allows a more detailed analysis for specific items of interest.

HARMONI is an AO-assisted IFS, which makes computation of achieved signal-to-noise complex. This is partly because the AO PSF varies strongly with wavelength over the HARMONI spectral range, but also because the size of the extraction aperture of scientific interest can vary depending on the science programme under consideration. For this document, we use two simple limiting cases for sensitivity computations:

1. A spatially uniform extended source with a size that is large compared to the telescope (+AO) PSF and large with respect to the atmospheric seeing.

2. An unresolved point source, for which we make the simple assumption that the extraction aperture is 2×2 spatial pixels in size at all wavelengths, for the HARMONI spaxel size adopted. If this spaxel size is rectangular, we increase extraction aperture to a square, i.e., for the 60×30 mas spatial scale we use a 120×120 mas extraction aperture.

The other parameters for the sensitivity computation are set as follows: The airmass for the observations is set at 1.3. ESO `Skycalc` (Version 2.0.9)[1], which is based on the Paranal Advanced Sky Model is used to determine the atmospheric transmission and sky background flux as a function of wavelength. Scattered light from sky lines is included as a 40% increase on the `Skycalc` [1] interline values (i.e. 20% increase in sky noise contribution), in keeping with the agreed instrument specification. For simulating the AO PSF for both LTAO and SCAO mode, we use the ESO standard 35-layer turbulence model and its Cn2 profile, a turbulence time constant (τ_0) of 5.35 ms, a seeing (r_0=15.7 cm) at 500 nm, and an outer scale for the turbulence of 25 m.

The telescope parameters are based on the current 39-m ELT design. After accounting for the M2 spiders, the effective maximum collecting area is 996 m^2, and the effective "all glass" collecting area is 929 m^2. To eliminate excess thermal background due to pupil wander in the telescope and instrument, we undersize the cold stop inside the IFS by 1%, reducing the effective collecting area further to 896 m^2. We use the undersized cold stop for all sensitivity estimates for all wavelengths longer than 1.0 μm, and the maximum collecting area for the other wavelengths.

For the telescope transmission we take the ESO specified values for the lateral port, and apply the aging correction as prescribed. This gives an ELT transmission of 82% at 2.2 microns. Telescope emissivity is computed as per the ELT Common ICD, which includes dust, segment gaps, and spider, but not the central obscuration. This gives an ELT emissivity of 23.3% at 2.2 microns. The apparent difference between emissivity and transmission comes from the masked areas of the pupil. Instrument induced thermal emission is separately calculated. For our sensitivity estimates we assume the median temperature of the telescope site of 282 K (+9°C).

Two different types of AO are considered, SCAO and LTAO. For both SCAO and LTAO, we use `TipTop` [3] within HSIM [4][8] to compute a PSF estimate, given the atmospheric parameters as described above, and guide star parameters that yield an AO PSF that meets the HARMONI image quality requirements for JQ2 in the respective AO modes. As the guide star parameters, i.e. brightness and off-axis distance, are degenerate, their exact values are not relevant, e.g. for LTAO mode we assume an off-axis guide star providing a total flux of 113.5 ph/m²/s at 55 arcsec off-centre distance, and for SCAO we assume an on-axis guide star providing a total flux of 32872.1 ph/m²/s. AO performance is scaled to models which meet the specified AO requirements. A small model-based degradation is then included to account for instrument effects.

4.1 Current Best Estimates

The tables below show the expected sensitivities derived using the current best estimates for instrument parameters such as throughput and image quality, rather than the contractual minimum performance, as the latter can be overly pessimistic. The instrument thermal background is based on the current optical design, operational temperatures (i.e. +2 °C in the FPRS/NGSS), and contamination models. The best estimate values vary as a function of operational mode, due to the different dichroics present in the light path. All optical elements within the IFS are assumed to be at a cryogenic temperature of 130 K, and while their contribution to the instrument background is included in the thermal model, their contribution is negligible.

By far the biggest contributor to the instrument's sensitivity is the detector performance in terms of QE, read noise and dark current. For the H4RG near-IR detectors, we use a realistic best estimate based on the detectors procured for the ESO-VLT MOONS instrument, namely a QE of 90% at 1.2 μm, effective read out noise of 4.5 e^- in SUTR mode for the 900 s exposure, and 15 e^-/hr dark current. For all spectral wavebands we account for sky-subtraction noise by simply doubling the background and read-noise contribution in our SNR calculation. We assume an equal amount of observing time is spent on the sky-observations, either by nodding on IFU or offsetting to sky, both strategies are the current baseline for sky-subtraction in HARMONI.

Sensitivities are reported in the tables are given at specific wavelengths defined to lie in known "dark" areas of the infrared sky. Each window's central wavelength is tabulated next to the grating setting. In the K band window, where the dominant thermal background has a strong wavelength dependence, we quote the sensitivities at a number of wavelengths within the K band.

4.2 Point source sensitivities

The following table shows the limiting AB magnitude of a point source, for which a signal-to-noise ratio of 5 is achieved in 5 hours (20 exposures of 900 s), with the extraction aperture box size indicated at the head of each column. The box sizes are 2×2 spaxels for the 10×10 and 20×20 mas spaxel scales, with the source centered within the box. For the 60×30 spaxel scale, where the spaxel is rectangular, the extraction aperture is square, at 120×120 spaxels, whereas for the 4×4 mas scale, the box size is 3×3 spaxels, so as to enclose most of the PSF core. For noAO scales, the box sizes are matched to excellent and good seeing.

There are 3 grating families, LR (low resolution, R~3000), MR (medium resolution, R~7000), and HR (high resolution, R~17000), as well as the visible grating (VIS). Each row of the table quotes the sensitivity at a specific wavelength, whose value in microns is given next to the grating name. There are no SCAO values at 0.915 μm, as the SCAO dichroic does not transmit science light below 1.0 μm. Similarly, neither LTAO nor SCAO dichroics allow observing at visible wavelengths.

Table 1: HARMONI point source sensitivities in AB mags (5 hours, 5 sigma) for different spaxel scale and grating configurations.

	no AO		LTAO (JQ2)				SCAO (JQ2)			
Box size (mas)	240×240	480×480	12×12	20×20	40×40	120×120	12×12	20×20	40×40	120×120
VIS (0.700)	25.17	25.72	-	-	-	-	-	-	-	-
LR1 (0.915)	23.94	24.46	24.33	25.25	25.60	25.61	-	-	-	-
LR1 (1.19)	24.21	24.69	24.83	25.75	26.10	26.01	26.00	26.75	26.90	26.48
LR2 (1.63)	23.78	24.24	25.21	26.06	26.22	25.68	26.14	26.84	26.88	26.10
LR2 (2.20)	23.17	23.59	25.02	25.39	25.17	24.37	25.80	26.08	25.74	24.77
LR2 (2.34)	22.52	22.94	24.50	24.72	24.45	23.65	25.25	25.39	25.00	24.04
MR1 (0.915)	21.82	22.23	23.76	24.68	25.06	25.15	-	-	-	-
MR2 (1.19)	23.49	24.00	24.13	25.06	25.43	25.42	25.30	26.05	26.23	25.89
MR3 (1.63)	23.62	24.11	24.65	25.54	25.78	25.34	25.58	26.32	26.44	25.76
MR4 (2.07)	23.44	23.89	24.59	25.34	25.34	24.63	25.39	26.04	25.92	25.03
MR4 (2.20)	22.77	23.19	24.48	24.99	24.81	24.03	25.26	25.67	25.38	24.43
MR4 (2.34)	22.18	22.60	24.10	24.40	24.14	23.35	24.85	25.06	24.70	23.74
HR1 (0.915)	21.52	21.93	22.73	23.66	24.06	24.24	-	-	-	-
HR2 (1.63)	22.59	23.10	23.68	24.61	24.95	24.68	24.62	25.39	25.61	25.09
HR3 (2.07)	22.79	23.24	23.68	24.55	24.70	24.11	24.48	25.25	25.29	24.51
HR4 (2.20)	22.24	22.67	23.59	24.30	24.24	23.51	24.36	24.98	24.81	23.90
HR4 (2.34)	21.66	22.08	23.39	23.86	23.66	22.88	24.13	24.52	24.21	23.27

4.3 Extended line source sensitivities

The tables below give the surface brightness in $W \cdot m^{-2} \cdot arcsec^{-2}$ for an infinitely extended source for a spectrally unresolved emission line. The surface brightness limits are independent of image quality and hence apply to all operating modes. The 'Current Best Estimate' value is given for the noAO transmission and thermal background values. The limits are given for an SNR of 5 per spectral resolution element, i.e. 2 detector pixels, over a 2×2 spaxel, with an on-source exposure time of 5 hours (20×900 s). As is the case for point sources, these surface brightness sensitivities account for sky-subtraction noise by simply doubling the background and read-noise contribution in our SNR calculation. We assume an equal amount of observing time is spent on the sky observations, typically offsetting to sky.

Table 2: HARMONI extended source sensitivities (line flux $W/m^2/arcsec^2$) for various spaxel scale and grating configurations.

	Extended unresolved line source sensitivity			
Box size (mas)	12×12	20×20	40×40	120×120
LR1 (0.915)	4.4E-19	1.1E-19	2.9E-20	5.8E-21
LR1 (1.19)	3.2E-19	7.8E-20	2.1E-20	3.9E-21
LR2 (1.63)	2.1E-19	5.5E-20	1.8E-20	4.7E-21
LR2 (2.07)	1.6E-19	5.4E-20	2.3E-20	7.1E-21
LR2 (2.20)	1.8E-19	8.1E-20	3.8E-20	1.2E-20
LR2 (2.34)	2.7E-19	1.4E-19	6.8E-20	2.3E-20
MR1 (0.915)	3.5E-19	8.6E-20	2.2E-20	4.1E-21
MR2 (1.19)	2.8E-19	6.9E-20	1.8E-20	3.1E-21
MR3 (1.63)	1.6E-19	4.2E-20	1.2E-20	3.0E-21
MR4 (2.07)	1.4E-19	4.2E-20	1.6E-20	4.8E-21
MR4 (2.20)	1.4E-19	5.5E-20	2.4E-20	7.8E-21
MR4 (2.34)	1.8E-19	8.8E-20	4.2E-20	1.4E-20
HR1 (0.915)	4.0E-19	9.8E-20	2.5E-20	4.2E-21
HR2 (1.63)	1.7E-19	4.3E-20	1.2E-20	2.4E-21
HR3 (2.07)	1.4E-19	3.9E-20	1.3E-20	3.4E-21
HR4 (2.20)	1.4E-19	4.6E-20	1.8E-20	5.6E-21
HR4 (2.34)	1.6E-19	6.4E-20	2.9E-20	9.4E-21

5. CONCLUSIONS

HARMONI is the workhorse, AO assisted, visible and near-infrared integral field spectrograph for the Extremely Large Telescope. It provides a range of spaxel scales and spectral resolving powers, allowing the user to tailor the instrument setup to optimally suit the observations being carried out. The super-sensitive, exquisite angular resolution spectroscopy it will enable will lead to a huge leap in understanding the physical phenomena that underpin the formation and evolution of a wide range of astrophysical sources. The instrument simulator HSIM [4][8] allows the end user to quantitatively estimate the efficacy of the proposed observations, and to best exploit synergies with other facilities such as ALMA, JWST, SKA.

REFERENCES

[1] ESO Skycalc Tool, https://www.eso.org/observing/etc/bin/gen/form?INS.MODE=swspectr+INS.NAME=SKYCALC (July 2024).

[2] Grisdale, K., et al., "On the viability of determining galaxy properties from observations – I. Star formation rates and kinematics," Monthly Notices of the Royal Astronomical Society, 513 (3), 3906-3924 (2022).

[3] Neichel, B. et al., "TIPTOP: a new tool to efficiently predict your favorite AO PSF", Proc. SPIE, 11448, 114482T (2020)

[4] Pereira-Santaella, M. and Routledge, L., "HSIM," Github, 2021, https://github.com/HARMONI-ELT/HSIM (July 2024).

[5] Richardson, M., Routledge, L., Thatte, N., Tecza, M., Houghton, R.C.W., Pereira-Santaella, M., Rigopoulou, D., "Simulating gas kinematic studies of high-redshift galaxies with the HARMONI integral field spectrograph," Monthly Notices of the Royal Astronomical Society, 498 (2), 1891-1904 (2020)

[6] Thatte, N.A., et al., "HARMONI at ELT: overview of the capabilities and expected performance of the ELT's first light, adaptive optics assisted integral field spectrograph," Proc. SPIE., Vol. 12184, 12184-20 (2022).

[7] Thatte, N., et al., "HARMONI: the ELT's first-light near-infrared and visible integral field spectrograph," ESO Messenger, Vol. 182, 7-12 (2021).

[8] Zieleniewski, S., et al., "HSIM: a simulation pipeline for the HARMONI integral field spectrograph," Monthly Notices of the Royal Astronomical Society, 453 (4), 3754-3765 (2015).

[9] Kendrew, S., et al., "Simulated stellar kinematic studies of high redshift galaxies with the HARMONI Integral Field Spectrograph," Monthly Notices of the Royal Astronomical Society, 458 (3), 2405-2422, (2016).